



Special Feature: Metal Forming and Processing

Research Report

Measurement Methods for Flow Stress of Metallic Materials in Large Strain Range

Yasuhiro Yogo, Takamichi Iwata, Michiaki Kamiyama, Masatoshi Sawamura, Noritoshi Iwata and Takashi Ishikawa

Report received on Feb. 24, 2015

■**ABSTRACT**■ Two methods were developed for measuring a stress-strain curve. One is a ring compression test for thin sheet metals. Using this method, a stress-strain curve can be measured up to a strain of 1.0 considering the plastic anisotropy. The measurements were demonstrated with mild steel and high-tensile steel. The measured stress-strain curve was applied to a finite element simulation, and the accuracy improvement was confirmed in the thickness reduction during sheet metal forming. The other method is a high-pressure torsion test for bulk metals. With this method, due to very high hydrostatic stress, a specimen can be continuously deformed without fracture. This enables us to measure a stress-strain curve up to a strain of 10.0.

■**KEYWORDS**■ Stress-strain Curve, Ring Compression Test, High-pressure Torsion, Plastic Anisotropy, Large Strain

1. Introduction

Finite element method (FEM) simulation is an indispensable tool for improving part quality and reducing manufacturing costs in metal forming processes. Therefore, more accurate FEM results are always desired. We know that the stress-strain curve (SS curve) strongly affects the accuracy of the results. In order to implement the SS curve more precisely into FEM simulations, material testing methods that measure SS curves have been proposed. However, with existing testing methods for SS curves, it is not possible to cover a large strain range that is introduced in actual processes.

In sheet stamping processes, larger strains (i.e., 1.0) occur around die corners than in other areas. However, by tensile testing, a fracture appears before the strain reaches 1.0. In forging processes for bulk metals, the introduced strain exceeds 5.0 (500%), although there is no method for measuring SS curves up to such large strains.

In this paper, two new testing methods for SS curves are proposed. First, a new ring compression test is proposed for thin sheet metals that enables us to measure SS curves considering the anisotropy. This is reviewed in Sections 2 and 3. Second, a new method with high-pressure torsion (HPT) is developed for bulk

metals. With this method, it is possible to measure SS curves up to a strain of 10. This is described in Sections 4 and 5.

2. Ring Compression Test for Thin Sheet Metals

2.1 Review of the Ring Compression Test

Osakada et al. proposed a ring compression test for measuring SS curves.⁽¹⁾ This method is reviewed in the following:

1: A rigid-plastic FEM analysis of the ring compression test is performed. The dimensional ratio of the specimen is *outer ring diameter: inner ring diameter: height* = 6 : 3 : 2.

2: The relationship between the height reduction and the inner ring diameter during compression are obtained by FEM analysis under various friction coefficients. By comparison with the experimental result, the actual friction coefficient is identified.

3: FEM analysis is performed again with the identified friction coefficient from step 2. The averaged plastic friction coefficient from step 2. The averaged plastic equivalent strain $\bar{\epsilon}_{ave}$ is defined by Eq. (1). Here, $\bar{\epsilon}_i$ and V_i are the plastic equivalent strain and the volume of element (i), respectively.

$$\bar{\epsilon}_{ave} = \frac{\sum(\bar{\epsilon}_i \times V_i)}{\sum V_i} \quad (1)$$

Then, the equivalent stress $\bar{\sigma}$ is calculated by Eq. (2). Here, a , n , and m are the material parameters.

$$\bar{\sigma} = a \left(\bar{\varepsilon}_{ave} \right)^n \left(\bar{\varepsilon}_{ave} \right)^m \quad (2)$$

4: According to Eq. (3), the nominal compression stress p is defined with the calculated compression force P and an initial compression area A_0 . Subsequently, the constraint factor f is calculated by Eq. (4).

$$p = P / A_0 \quad (3)$$

$$f = p / \bar{\sigma} \quad (4)$$

5: According to Eq. (5), the averaged equivalent stress $\bar{\sigma}_{ave}$ is calculated with the measured compression force P_m .

$$\bar{\sigma}_{ave} = \frac{P_m}{A_0 \cdot f} \quad (5)$$

6: Using Eq. (1) and Eq. (5), the relationship between $\bar{\varepsilon}_{ave}$ and $\bar{\sigma}_{ave}$ (i.e., SS curve) is obtained.

7: Steps 1-6 are repeated until the difference between the previous SS curve and the present SS curve becomes small enough.

According to Osakada et al.,⁽¹⁾ the initial work hardening factor n and the initial strain-rate factor m in Eq. (2) have little effect on the obtained SS curves; however, the friction coefficient has a strong effect.

In our study, we developed a new ring compression test for thin sheet metals. The points of this test are as follows:^(2, 3)

An elastic-plastic body was defined as the die model in the FEM analysis.

- The reduction in height was measured by a video-type extensometer.
- A plastic anisotropy model (described in Section 2. 2) was incorporated.
- The appropriate dimension ratio for thin sheet metals was examined.

2. 2 Incorporation of Plastic Anisotropy

An SS curve measured with the ring compression test is under uniaxial compression. The SS curves of thin sheet metals are not identical to that under uniaxial tension because they have plastic anisotropy. The way to convert the result of the ring compression test to an SS curve under uniaxial tension is described

below. The equivalent stress based on the Hill'48 yield function⁽⁴⁾ is described by Eq. (6).

$$\bar{\sigma}^2 = F(\sigma_y - \sigma_z)^2 + G(\sigma_z - \sigma_x)^2 + H(\sigma_x - \sigma_y)^2 + 2L\sigma_{xy}^2 + 2M\sigma_{yz}^2 + 2N\sigma_{zx}^2 \quad (6)$$

The relationship between the compression stress $\sigma_{compression}$ and each stress component can be described as $\sigma_x = \sigma_y = \sigma_{xy} = \sigma_{yz} = \sigma_{zx} = 0$, $\sigma_z = \sigma_{compression}$. Equation (7) is derived by substituting these equations into Eq. (6).

$$\bar{\sigma}^2 = (F + G) \sigma_{compression}^2 \quad (7)$$

Equation (8) is obtained by substituting $F = r_0 / \{r_0(1 + r_0)\}$ and $G = 1 / (1 + r_0)$ for Eq. (7).

$$\bar{\sigma} = \sqrt{\frac{r_0 + r_{90}}{r_{90}(1 + r_0)}} |\sigma_{compression}| \quad (8)$$

Using Eq. (8), the SS curve under uniaxial compression obtained by the ring compression test can be converted to an SS curve under uniaxial tension.

2. 3 Measurement of SS Curves by the Ring Compression Test

A specimen was compressed up to a reduction in height of 65%, which is equivalent to a 1.0 true strain with a universal testing machine. A self-aligning seat was attached to the die to apply a uniform pressure. The height reduction, which is measured by the change in distance between markers on the upper and lower dies, was measured using a video-type extensometer. The configuration of the testing tools is shown in Fig. 1.

The sample materials are three kinds of steel grades,

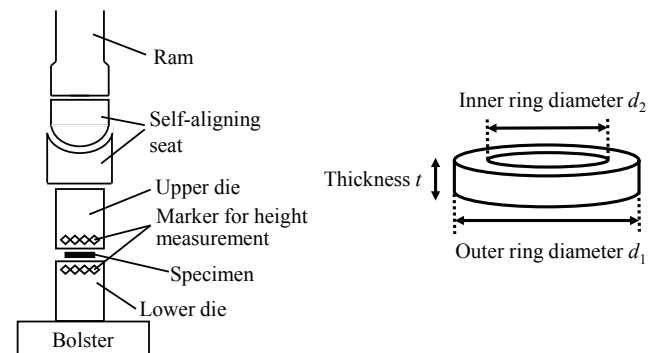


Fig. 1 Schematic diagram of experimental setup for the ring compression test.

as shown in **Tables 1** and **2**, and the dimensions of the specimens are shown in **Table 3**. The height direction of the specimen corresponded to the thickness direction of each steel sheet, and the dimension ratio of the specimen is *outer ring diameter* d_1 : *inner ring diameter* d_2 : *thickness* $t = 4 : 2 : 1$. The dimensions of the inner and outer ring diameters were measured by a stereoscopic microscope before and after testing.

3. Evaluation of SS Curves by Ring Compression Test

3.1 Verification of SS Curves

The SS curves for mild steel SCGA270D measured by the tensile test, the hydraulic bulge test, and the developed ring compression test are shown in **Fig. 2**. The ring compression test was performed twice, and both results (N1 and N2) are shown in Fig. 2. The SS curves from the ring compression test are coincident with that from the hydraulic bulge test. On the other

hand, the SS curves from the ring compression test were higher than the extrapolated curve based on the tensile test with the Nth power hardening law⁽⁵⁾ in Eq. (9). The difference is due to the plastic anisotropy.

$$\sigma = F (\varepsilon + \varepsilon_0)^n \tag{9}$$

The SS curves from the ring compression test and the hydraulic bulge test are converted to the uniaxial stress condition using Eq. (8) in **Fig. 3**. All SS curves show

Table 1 Mechanical properties of sheet metals.

	YS [MPa]	TS [MPa]	El [%]	Thickness [mm]
SCGA270D	125	283	44.6	0.70
SPC590DU	337	619	28.6	1.20
SPC980DU	843	1030	15.5	1.20

Table 2 Rankford values.

	r_0	r_{45}	r_{90}
SCGA270D	1.60	1.36	1.90
SPC590DU	0.83	0.92	0.85
SPC980DU	0.89	0.94	1.15

Table 3 The dimensions of the ring compression test specimens.

	Outer ring diameter d_1 [mm]	Inner ring diameter d_2 [mm]	Thickness t [mm]
SCGA270D	1.4	2.8	0.7
SPC590DU	2.0	4.0	1.0
SPC980DU	2.0	4.0	1.0

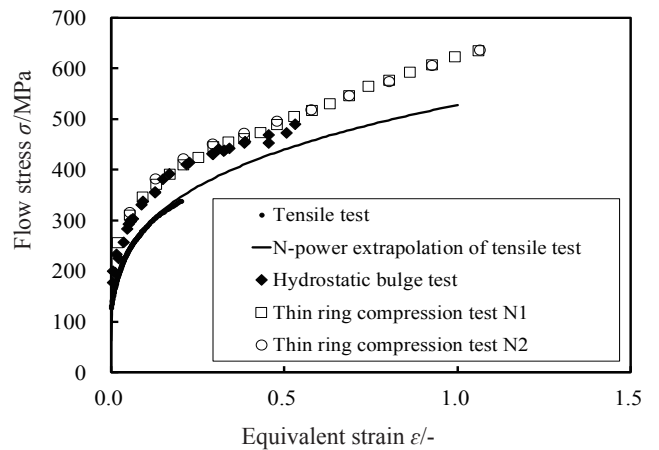


Fig. 2 SS curves of SCGA270D without consideration of plastic anisotropy.

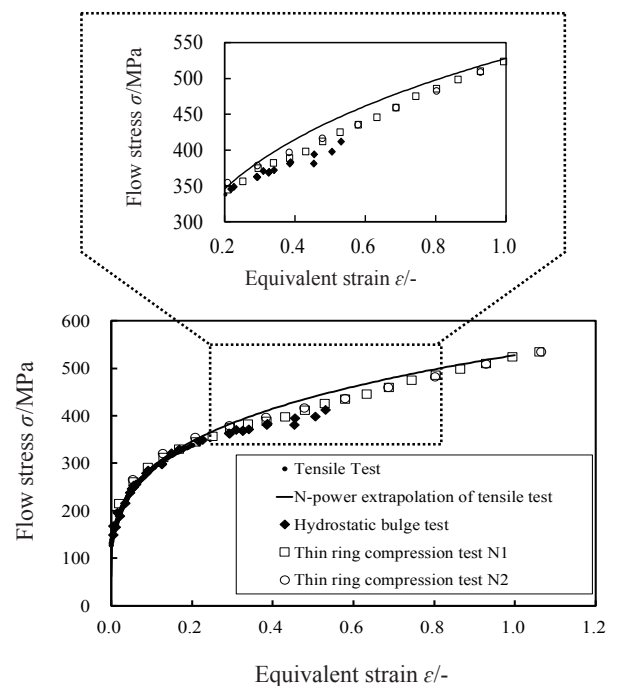


Fig. 3 SS curves of SCGA270D with consideration of plastic anisotropy.

good correspondence up to a strain of 0.3. However, a difference appeared between the SS curve from the ring compression test and the extrapolated curve over a strain of 0.3.

It is demonstrated that SS curves can be measured with high-strength steel using the ring compression test in Fig. 4. Over a strain of 0.5, the SS curves from the ring compression test are nearly a straight line and are higher than the extrapolated curves from the tensile test.

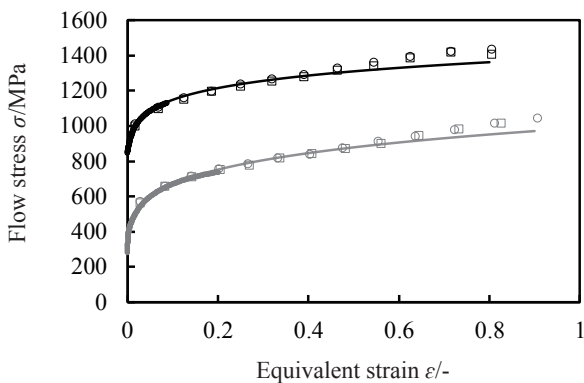
3.2 Application of Measured SS Curve to a Bulging Test

A simulation of a bulging test was performed with the SS curve from the ring compression test and with the extrapolated SS curve to compare the thickness reduction because it has been recognized that the forming limit in a bulging test is strongly affected by the plastic hardening⁽⁶⁻⁸⁾ behavior in SS curves. The bulging test was performed with the tools in Fig. 5. The tool material and the specimen were SKD11 (a typical tool steel) and SCGA270D, respectively. The lubricant on the specimen was a rust-preventing oil. The triangular bead was fabricated onto the blank holder, and the blank holder force was 10 tonf to

prevent material flow on the flange surface.

FEM analysis of the bulging test was performed with the configuration shown in Fig. 5. LS-DYNA was used as the FEM analysis solver, and JSTAMP/NV was used as the pre/post processor. The friction coefficient in the simulation was 0.135, which was measured by a slide-type friction test under the same conditions as the bulging test. The simulations were performed using the SS curve from the ring compression test and the extrapolated SS curve.

An overview of the specimen and the calculated thickness distribution are shown in Fig. 6. The relationship between the punch stroke and the logarithmic strain in the thickness direction was compared with the FEM analysis in Fig. 7. The thickness distribution along the rolling direction was measured with a dial gauge, and the logarithmic strain in the thickness direction in Fig. 7 was defined as the smallest measured thickness. The logarithmic strain in the thickness direction calculated in the FEM analysis with the SS curve from the ring compression test corresponds with the experimental results.



- SPC590DU (Tensile test)
- SPC590DU (N-power extrapolation of tensile test)
- SPC590DU (Ring compression test N1)
- SPC590DU (Ring compression test N2)
- SPC980DU (Tensile test)
- SPC980DU (N-power extrapolation of tensile test)
- SPC980DU (Ring compression test N1)
- SPC980DU (Ring compression test N2)

Fig. 4 SS curves of SPC590DU and SPC980DU.

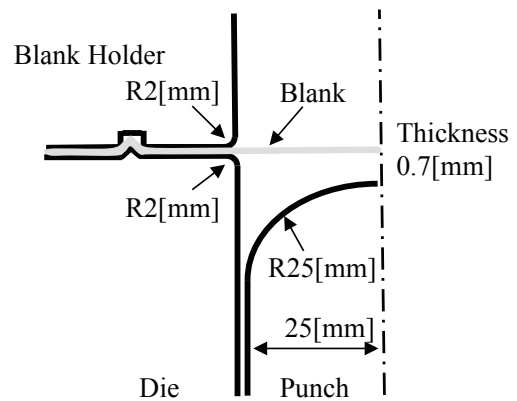


Fig. 5 Schematic diagram of the bulging test.

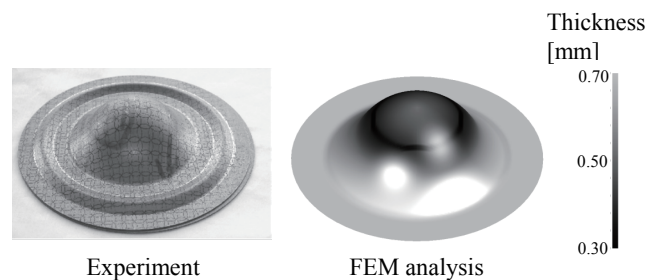


Fig. 6 Experiment and FEM analysis of the bulging test.

In contrast, the logarithmic strain in the thickness direction from the FEM analysis with the extrapolated SS curve was smaller than the experimental result over a logarithmic strain of 0.2 in the thickness direction. This is due to the plastic hardening behavior of the SS curve for the extrapolated curve based on the Nth power law being larger than that of the ring compression test curve. In conclusion, it is important that the SS curve is measured up to the strain introduced in the actual forming process to predict the thickness reduction accurately in the FEM analysis, and it was demonstrated that the ring compression test was useful for the measurement.

4. HPT Test for Bulk Metals

Next, a new method for bulk metals is proposed to measure SS curves up to a strain of 10 (1000%).

4.1 HPT Test

High-pressure torsion was applied for the measurement. Due to the high pressure, the specimen can be continuously strained without breaking.^(9,10) The material used for the specimens was pure aluminum (99.9%). The specimen was a disc 1 mm in thickness and 10 mm in diameter, and the experimental setup is shown in **Fig. 8**. All of the surfaces of the specimen were enclosed by the upper and lower dies and the ring. Therefore, the specimen dimensions did not change during HPT testing. In order to suppress sliding between the specimen and the upper and lower dies, small hollows and grooves were machined into the contacting surfaces of the upper and lower dies.

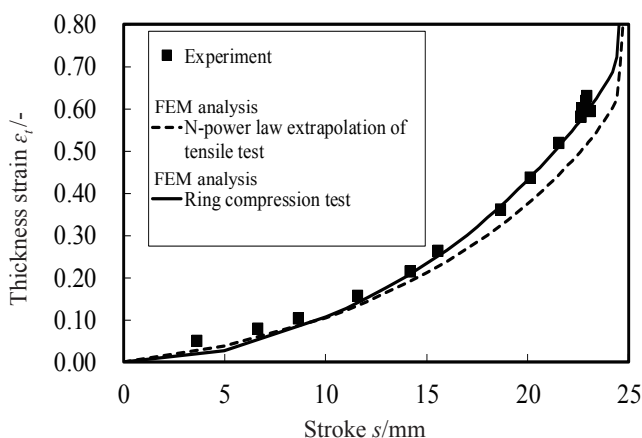


Fig. 7 Comparison of thickness strain.

The specimen was compressed at 1 GPa between the dies and was subsequently torsionally strained by the rotation of the upper die. The rotation speed of the upper die was 1 rpm. The compression load, rotation angle, and torque of the upper die were measured during the test at room temperature.

4.2 Measurement of Actual Rotation Angle of a Specimen in the HPT Test

The specimen is torsionally strained by the rotation of the upper die. As reported by Edalati et al., the rotation angle of the upper die is not always the same as that of the specimen due to slippage.⁽¹¹⁾ Therefore, the actual rotation angle of the specimen after HPT testing should be measured to accurately determine the introduced strain. Thin copper (Cu) foil was inserted in two semi-circular specimens, and the foil thickness was 0.05 mm. After testing, the torsion angle of the Cu foil was measured from both the front and back views.

5. Determination Procedure for SS Curve

5.1 Torque and Torsion Angle

The measured compression load and torque are shown in **Fig. 9**. The measured torque shows a drastic increase at the beginning followed by an almost constant value. The compression force can be maintained at a constant value during the entire HPT test.

The torsion angle of the specimen was measured

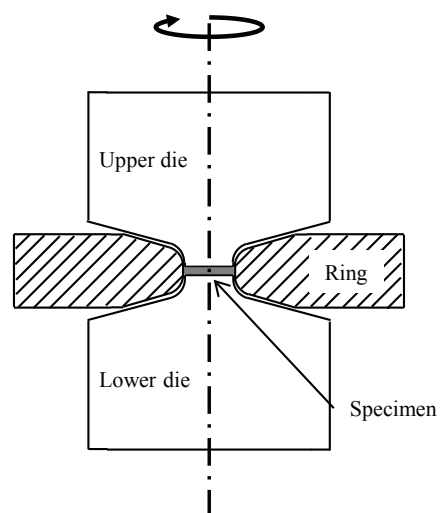


Fig. 8 Schematic diagram of the experimental setup for the HPT tests.

using the inserted Cu foil from both the front and back views. The relationship between the rotation angle of the upper die and the torsion angle of the specimen is shown in Fig. 10. From 0 to 45 degrees of rotation of the upper die, no slippage occurred between the specimen and the upper die. Beyond that, a small slippage of about 20 degrees occurred.

5.2 Strain

The way to convert the rotation angle of the upper die into strain is discussed in this section. In order to investigate the relationship between the rotation angle of the upper die and the average strain throughout the specimen, the calculated results from the FEM simulations were averaged using Eq. (1). It is possible

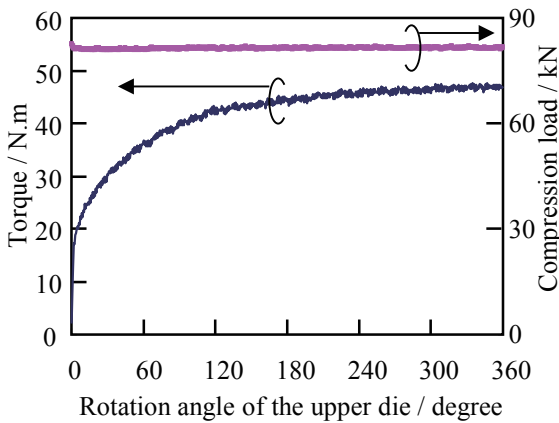


Fig. 9 Torque and compression load measured in an HPT test.

to obtain the relationship between the rotation angle of the upper die and the actual average strain of a specimen by combining Fig. 10 and ϵ_{ave} . The relationship obtained is shown in Fig. 11.

5.3 Stress

Osakada proposed a procedure to convert the compression load into an SS curve using compression testing.⁽¹²⁾ His theory was modified to measure the SS curve using HPT testing. First, an FEM calculation was conducted using a fictitious material with an SS curve described by Eq. (10).

$$\sigma = \epsilon^{0.001} \tag{10}$$

Using the calculation results, the average strain and restraint factor f were calculated using Eqs. (11) and (12), respectively.

$$\sigma_{ave} = \frac{\sum_i V_i \sigma_i}{\sum_i V_i} \tag{11}$$

$$f = \frac{T_{FEM}}{\sigma_{ave}} \tag{12}$$

Here, σ_{ave} is the average stress in the specimen, σ_i is the equivalent stress of element (i), and T_{FEM} is the calculated torque. By combining the measured torque and the calculated restraint factor f , an SS curve is obtained using Eq. (13).

$$\sigma = \frac{T_{exp}}{f} \tag{13}$$

Here, T_{exp} is the measured torque. Using the obtained

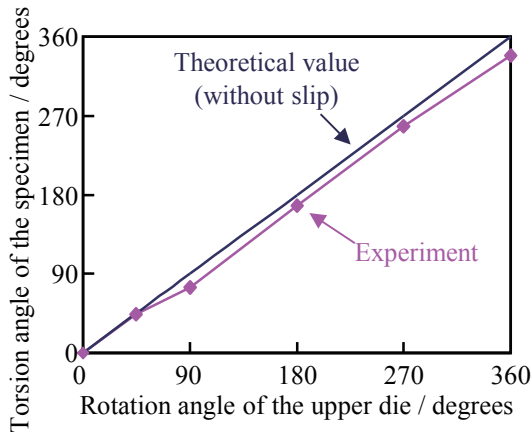


Fig. 10 Relationship between the rotation angle of the upper die and the torsion angle of a specimen.

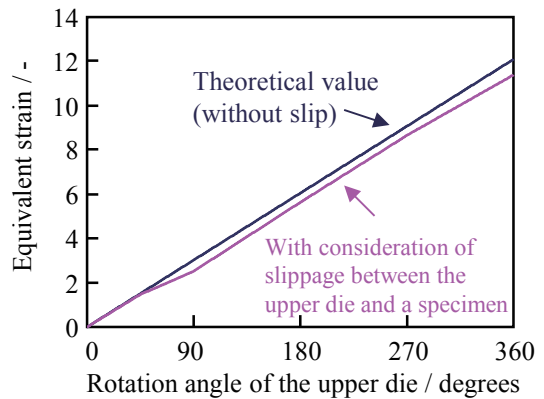
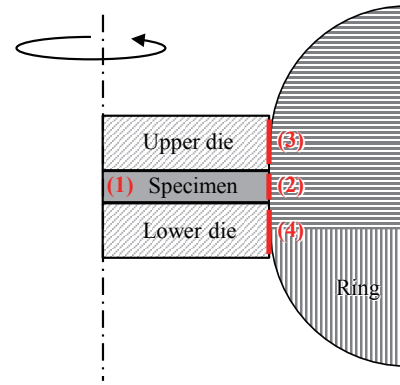


Fig. 11 Relationship between the rotation angle of the upper die and the average strain in a specimen.

SS curve, this procedure was repeated until the difference between the formerly defined stress and the obtained stress became small enough. The obtained SS curve is shown in Fig. 12. The measurement was conducted twice, and the results are indicated as N = 1 and 2 in Fig. 12.

An SS curve was also measured by a compression test,⁽¹²⁾ and the measured SS curve obtained is shown in Fig. 12. There is a large discrepancy between the two curves. The SS curve is based on the measured torque in the HPT test, and the discrepancy appeared because of this measurement. In order to evaluate an SS curve using the HPT test, only the torque from the torsional deformation of the specimen should be used. However, as shown in Fig. 13, other factors ((2) to (4)) were included in this measurement. It is very difficult to eliminate the effect of the other factors when measuring torque. Therefore, the difference in yield stress is recognized as the effect of the other factors. Here, it is assumed that the other factors caused by the friction force are at a constant value throughout the measurement. By eliminating the effect of the other factors, as shown in Fig. 14, the SS curve was modified, and the modified SS curve is shown in Fig. 15. It is shown that the SS curve was successfully measured for strains up to 10.0. In addition, the SS curve obtained using the HPT test shows good correlation with that obtained by compression testing up to a strain of 1.0. It is natural that both of the yield stresses are the same. However, the work-hardening behavior of the HPT test corresponds with that of the compression test. This result shows the validity of the measured results for the developed method.



$$\text{Measured torque} = (1) + (2) + (3) + (4)$$

- (1): Torque due to torsional deformation of a specimen.
- (2): Torque due to the friction force between a specimen and the ring.
- (3): Torque due to the friction force between the upper die and the ring.
- (4): Torque due to the friction force between the lower die and the ring.

Fig. 13 Schematic diagram of the influence of the friction forces on the measured torque.

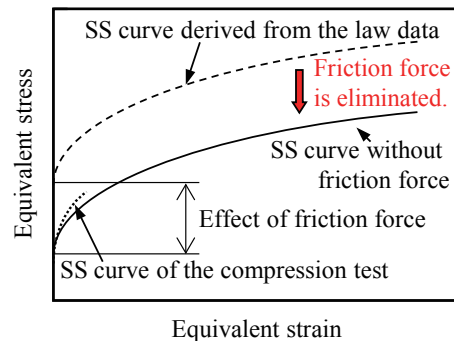


Fig. 14 Schematic diagram showing the elimination of torque due to the friction forces from the measured torque.

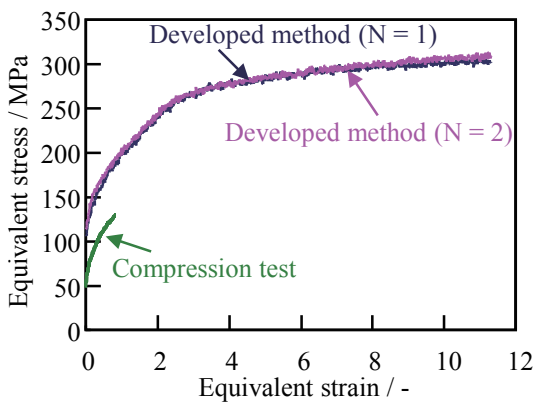


Fig. 12 Comparison of SS curves between the developed method and a compression test.

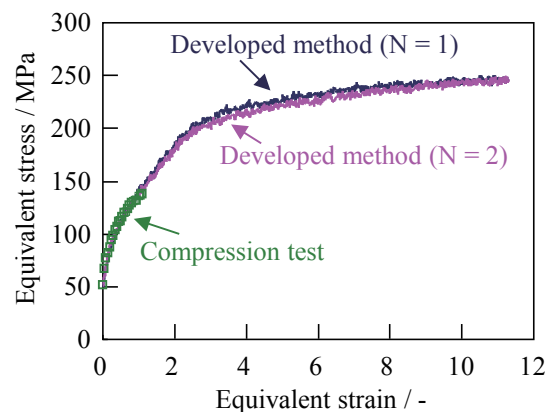


Fig. 15 Comparison of SS curves between the developed method and a compression test.

6. Summary

In our study, two methods were proposed for measuring SS curves: the ring compression test for thin sheet metals and the HPT test for bulk metals. Using those methods, the following results were obtained:

(1) The measurement method for the SS curve using the ring compression test was proposed for thin sheet metals, and the method for considering plastic anisotropy was also examined. As a result, the SS curves of the thin sheet metals were measured in a large strain range.

(2) It is demonstrated that SS curves can be measured for mild steel and high-strength steels using the ring compression test. The SS curves from the ring compression test were compared with the extrapolated SS curve from the tensile test. All of the SS curves showed good correspondence up to a strain of 0.3. However, a discrepancy appeared over a strain of 0.3.

(3) As shown in the bulging simulation with the SS curves from the ring compression test, the predictability of the thickness strain improved compared with the extrapolated curve. Based on this result, it was confirmed that the ring compression test was useful for measuring SS curves.

(4) A method was proposed for measuring the SS curve of a bulk metal in a super-large strain range. In the developed method, HPT was applied. It was shown that an SS curve was successfully measured for strains up to 10.0. In addition, the SS curve obtained using the developed method showed good correlation with that from compression testing up to a strain of 1.0.

References

- (1) Osakada, K. et al., *Trans. JSME C* (in Japanese), Vol. 55, No. 516 (1989), pp. 2213-2220.
- (2) Iwata, T. et al., *J. JSTP* (in Japanese), Vol. 54, No. 632 (2013), pp. 836-840.
- (3) Iwata, T. et al., *J. JSTP* (in Japanese), Vol. 54, No. 632 (2013), pp. 841-845.
- (4) Hill, R., *Proc. Roy. Soc. London*, Vol. A193 (1948), pp. 281-297.
- (5) Swift, H. W., *J. Mech. Phys. Solids.*, Vol. 1 (1952), pp. 1-18.
- (6) Swift, H. W., *Sheet Metal Ind.*, Vol. 31, No. 330 (1954), pp. 817-828.
- (7) Kawai, N. et al., *Trans. JSME* (in Japanese), Vol. 67, No. 542 (1964), pp. 431-439.
- (8) Kawai, N. et al. *Trans. JSME* (in Japanese), Vol. 40, No. 338 (1974), pp. 2956-2965.
- (9) Bridgman, P. W., *Studies in Large Plastic Flow and Fracture with Special Emphasis on the Effects of Hydrostatic Pressure* (1952), McGraw-Hill.
- (10) Zhilyaev, A. P. et al., *Acta Mater.*, Vol. 51, No.3, (2003), pp. 753-765
- (11) Edalati, K. et al., *Scripta Materialia*, Vol. 60, No. 1 (2009), pp. 9 -12
- (12) Osakada, K. et al., *CIRP Annals - Manufacturing Technology*, Vol. 30, No. 1 (1981), pp. 135-139

Figs. 1-7 and Tables 1-2

Reprinted from *J. JSTP*, Vol. 54, No. 632 (2013), pp. 841-845, Iwata, T., Yogo, Y., Iwata, N., Kato, S., Ishikawa, T. and Suzuki, K., Flow Stress Measurement Considering Plastic Anisotropy of Steels: Measurement Method for Flow Stress in Large Strain Range for Thin Sheet Metals (2nd report), © 2013 The Japan Society for Technology of Plasticity, with permission from JSTP.

Figs. 8-15

Reprinted from *Mat. Sci. & Eng. A*, Vol. 600 (2014), pp. 82-89, Yogo, Y., Sawamura, M., Hosoya, M., Kamiyama, M., Iwata, N. and Ishikawa, T., Measurement Method for Stress-strain curve in a Super-large Strain Range, © 2014 Elsevier, with permission from Elsevier.

Yasuhiro Yogo

Research Fields:

- Metal Forming
- Heat Treatment
- Physical Metallurgy
- CAE

Academic Degree: Dr.Eng.

Academic Societies:

- The Japan Society for Technology of Plasticity
- The Iron and Steel Institute of Japan

**Takashi Ishikawa***

Research Field:

- Metal Forming

Academic Degree: Dr.Eng.

Academic Societies:

- The Japan Society for Technology of Plasticity
- The Iron and Steel Institute of Japan
- The Japan Institute of Metals and Materials
- The Japan Society for Precision Engineering
- The Japan Institute of Light Metals

Awards:

- JSTP Best Paper Awards, The Japan Society for Technology of Plasticity, 1978
- JSTPAIDA Awards, The Japan Society for Technology of Plasticity, 1990
- Academic Prize of Nishiyama Medal, The Iron and Steel Institute of Japan, 1996
- JSTP Aida Medal, The Japan Society for Technology of Plasticity, 2004
- ISIJ Scientific Achievement Merit Prize, 2006
- JSHT Best Paper Awards, The Japan Society for Heat Treatment, 2011

**Takamichi Iwata**

Research Fields:

- Sheet Metal Forming Simulation
- Material Testing

Academic Societies:

- The Japan Society for Technology of Plasticity
- The Iron and Steel Institute of Japan

**Masatoshi Sawamura**

Research Fields:

- Metal Forming
- Tribology

Academic Society:

- The Japan Society for Technology of Plasticity

**Michiaki Kamiyama**

Research Fields:

- Metal Forming
- Tribology

Academic Societies:

- The Japan Society for Technology of Plasticity
- The Iron and Steel Institute of Japan

**Noritoshi Iwata**

Research Field:

- Metal Forming

Academic Degree: Dr.Eng.

Academic Society:

- The Japan Society for Technology of Plasticity



* Nagoya University